



CHORUS

This is the accepted manuscript made available via CHORUS. The article has been published as:

Kaluza-Klein graviton phenomenology for warped compactifications, and the 750 GeV diphoton excess

Steven B. Giddings and Hao Zhang

Phys. Rev. D **93**, 115002 — Published 1 June 2016

DOI: [10.1103/PhysRevD.93.115002](https://doi.org/10.1103/PhysRevD.93.115002)

Kaluza-Klein graviton phenomenology for warped compactifications, and the 750 GeV diphoton excess

Steven B. Giddings and Hao Zhang

Department of Physics, University of California, Santa Barbara, California 93106, USA

A generic prediction of scenarios with extra dimensions accessible in TeV-scale collisions is the existence of Kaluza-Klein excitations of the graviton. For a broad class of strongly-warped scenarios one expects to initially find an isolated resonance, whose phenomenology in the simplest cases is described by a simplified model with two parameters, its mass, and a constant Λ with units of mass parameterizing its coupling to the Standard Model stress tensor. These parameters are in turn determined by the geometrical configuration of the warped compactification. We explore the possibility that the 750 GeV excess recently seen in 13 TeV data at ATLAS and CMS could be such a warped Kaluza-Klein graviton, and find a best-fit value $\Lambda \approx 60$ TeV. We find that while there is some tension between this interpretation and data from 8 TeV and from the dilepton channel at 13 TeV, it is not strongly excluded. However, in the simplest scenarios of this kind, such a signal should soon become apparent in both diphoton and dilepton channels.

I. INTRODUCTION

One fascinating possibility for physics at or near the TeV scale is that of gravity in extra dimensions. Depending on the geometry of the extra dimensions, such a scenario can predict new relations[1] between the fundamental Planck scale, where gravity becomes strongly coupled, and the weak scale, shedding new light on the hierarchy problem. A generic feature of these scenarios is the presence of Kaluza-Klein (KK) excitations of the graviton, which could be a first signature of such physics.

An excess in the diphoton invariant mass spectrum has recently been reported by both the ATLAS and CMS collaborations at the 13 TeV LHC [2, 3], prompting a flood of ≈ 200 papers proposing its interpretation.¹ However, most of these have focussed on the case of a spin-zero resonance (though [5–11] consider aspects of spin-two resonances).

In particular, it was argued in [5] that a minimal KK graviton scenario is ruled out by the absence of a dilepton signal.² However, given the significant implications and interest if the 750 GeV excess were the signal of extra dimensions, it is worth taking a careful look at this interpretation and bounds on it. This is one focus of this paper. At the same time, we describe a simple and natural way to discuss the phenomenology of a KK graviton from a generic extra-dimensional scenario. In general, such scenarios will be “warped;” a simplest example of this phenomenon is exhibited in the Randall-Sundrum model[13], but much more general possibilities exist in extra-dimensional theories such as string theory. Indeed, if the 750 GeV excess is a KK graviton, the presence of an isolated resonance at this mass scale would indicate a strongly warped scenario, as opposed to one with purely

large extra dimensions[1, 14]. We describe a simple and general parameterization of general warped compactifications, and of the phenomenology of their KK graviton modes. In particular, the low-energy phenomenology of the simplest models – with a warped metric and SM matter concentrated at a single point in the extra dimensions – is naturally described in terms of the mass of the lightest KK graviton, and a single parameter Λ with mass dimension one, which characterizes the minimal coupling of this KK graviton to the stress tensor of Standard Model (SM) matter.

This paper will explore the interpretation of the LHC13 data as fixing the value of this coupling parameter, and will examine other constraints on it. We find that the combined 13 TeV excess gives $\Lambda \approx 60$ TeV, and while other constraints begin to have tension with this, such a coupling strength is not strongly ruled out. Also, in the simple example of the Randall-Sundrum model, the relevant parameters are apparently not ruled out by the absence of a radion signal, since the radion is expected to be light (< 4 GeV) and very weakly coupled. In turn, in the simplest warped compactification models, the coupling Λ determines the value of the higher-dimensional Planck mass. We also find that, again in the simplest models, such a value for Λ should be confirmed, or ruled out, in both the upcoming diphoton data and in that for dileptons.

II. WARPED COMPACTIFICATIONS AND TEV(ISH)-SCALE GRAVITY

A. General warped compactifications

Generic extra-dimensional configurations, *e.g.* in string theory, are warped, due to the possible presence of frozen-in fluxes and branes. This means that the D -dimensional spacetime metric takes the form

$$ds^2 = e^{2A(y)} dx_4^2 + g_{ab}(y) dy^a dy^b, \quad (1)$$

¹ For an recent extensive list, see [4].

² The *Particle Data Book* [12] also states a lower bound on KK gravitons of ~ 2 TeV, but this bound is strongly parameter dependent.

where A is a function of the $n = D - 4$ compact coordinates y^a , dx_4^2 is our four-dimensional, nearly-Minkowski metric, and g_{ab} are the compact components of the metric. Such compactifications can lead to interesting new explanations for the relative sizes of the fundamental Planck scale, the four-dimensional Newton's constant, and the weak scale. In particular, if M_D is the D -dimensional Planck scale, then the four-dimensional Planck scale, $M_4 \simeq 2.4 \times 10^{18}$ GeV, related to Newton's constant by $M_4^2 = 1/(8\pi G_N)$, is given by³

$$\frac{M_4^2}{M_D^2} = V_W \left(\frac{M_D}{2\pi} \right)^{D-4} \quad (2)$$

where

$$V_W = \int d^n y e^{2A(y)} \sqrt{g(y)} \quad (3)$$

is called the *warped volume*. From (2) one sees that the fundamental Planck scale M_D can be in the TeV range – so with large ratio M_4/M_D – either due to large warp factor e^A , or to large volume $\int d^n y \sqrt{g}$, or to some combination of the two. This recasts the hierarchy problem as one of explaining the large warped volume.

Limiting cases are the large-extra dimensions scenarios of Arkani-Hamed, Dimopoulos, and Dvali[1, 14], and the toy warped model of Randall and Sundrum[13], but a continuum of possibilities exist. In the simplest scenarios, SM matter is taken to reside on a $3 + 1$ dimensional subspace of the full geometry, commonly defined by a brane such as the D-branes of string theory, although extra-dimensional structure for gauge fields and matter is also possible.

If M_D is in a range near the TeV scale, a variety of important new prospects for phenomenology present themselves; one can in particular find new states below M_D arising as higher-dimensional Kaluza-Klein modes. For example in the large-radius [1, 14] limiting case, with vanishing warping A and a toroidal compact manifold, these KK modes have masses $m_{KK} \sim 1/R_i$ where R_i are the radii of the torus. More generally the KK masses are determined by characteristic radii of curvature of the geometry, so may depend on the geometry of g_{ab} and/or on the variation scale of the warp factor $A(y)$. This means it is useful to parameterize such phenomenology simply by the lightest KK graviton mass, m_1 , which can have complicated dependence on the internal geometry. There can be other modes in a similar mass range, such as four-dimensional scalars arising from low-energy modes of g_{ab} in the extra dimensions; these moduli modes include the “radion,” arising from an overall rescaling of the internal metric.

For the time being we focus on phenomenology of the lightest KK graviton. This state can be described by expanding the four-dimensional part of the metric as

$$g_{\mu\nu}(x, y) = e^{2A(y)} [\eta_{\mu\nu} + \kappa h_{\mu\nu}(x, y)] \quad (4)$$

where $\kappa^2 = (2\pi)^{D-4}/M_D^{D-2}$ gives the gravitational coupling, and the expansion of the metric perturbation in KK modes is

$$h_{\mu\nu}(x, y) = \sum_{N=0}^{\infty} h_{N\mu\nu}(x) \phi_N(y) . \quad (5)$$

$\phi_N(y)$ are the internal wavefunctions of the KK modes, and $N = 0$, with constant wavefunction, gives the 4d graviton. In the simplest scenarios, focussing on the graviton yields significant predictivity, since in these scenarios gravitons universally couple to the stress tensor $T_{\mu\nu}$ of the SM. In particular, consider a higher-dimensional lagrangian including the Einstein-Hilbert term and SM matter localized on the brane,

$$S = \frac{M_D^{D-2}}{(2\pi)^{D-4}} \int d^D X \sqrt{-g} \frac{\mathcal{R}}{2} + \int d^D X \sqrt{-g} \delta^n(y) \mathcal{L}_{\text{SM}} + \dots \quad (6)$$

with $\delta^n(y)$ localizing to $y^a = 0$. We choose the scale of x^μ to set $A(0) = 0$. If one chooses to normalize ϕ_1 so $h_{1\mu\nu}$ has a 4d canonical kinetic term, one finds a four-dimensional interaction lagrangian

$$\mathcal{L}_1 = -\frac{1}{\Lambda} h_{1\mu\nu}(x) T^{\mu\nu}(x) . \quad (7)$$

Here the dimension-one constant Λ is given by the gravitational coupling κ and the wavefunction ϕ_1 at the Standard Model location $y^a = 0$,

$$\Lambda = \frac{2}{\kappa \phi_1(0)} = M_D \left(\frac{M_D r_1}{2\pi} \right)^{n/2} . \quad (8)$$

In the last equality a simple parameterization of the extra-dimensional wavefunction is introduced as a radius, $\phi_1(0) = 1/r_1^{n/2}$; this radius r_1 characterizes the typical density of the KK wavefunction near the brane.

The bottom line is simple: the couplings of the lowest KK graviton to SM fields may be parameterized by a single mass scale Λ , and in the simplest scenarios this state's phenomenology is largely determined by this parameter and its mass m_1 . We treat these as free parameters, though return to comment on their possible sizes later; one can think of this as defining a “simplified model” for KK graviton phenomenology.

B. The Randall-Sundrum model

The Randall-Sundrum two-brane model [13] RS1 provides an illustrative toy model of the preceding discussion. It may be described by a five-dimensional metric (compare (1))

$$ds^2 = e^{2ky} dx_4^2 + dy^2 \quad (9)$$

³ Herein we mainly use the conventions of the large extra dimensions section of [12], which differ from those of the warped extra dimensions section; for related broad discussion of warped compactification parameters see [15].

where y ranges from 0 (“IR” or “SM brane”) to πR (“UV brane”). This differs from the original parameterization[13] in terms of coordinates x', ϕ by

$$x' = e^{\pi k R} x \quad , \quad \phi = \pi - y/R ; \quad (10)$$

in [13] R was called r_c . Then, the four- and five-dimensional Planck masses are related by (compare (2))

$$M_4^2 = \frac{M_5^3}{2\pi} \int_0^{\pi R} dy e^{2ky} = \frac{M_5^3}{4\pi k} (e^{2\pi k R} - 1) . \quad (11)$$

The mass of the lowest graviton KK mode is [16]

$$m_1 = x_1 k \quad (12)$$

where $x_1 = 3.83$ is the first zero of the Bessel function J_1 . The parameter k also determines the falloff radius $r_1 \propto 1/k$, so we find[16] (compare (8))

$$\Lambda = \frac{M_5}{2} \sqrt{\frac{M_5}{4\pi k}} (1 - e^{-2\pi k R}) \simeq M_5 \sqrt{\frac{M_5}{16\pi k}} \quad (13)$$

since typically $kR \gg 1$. In this RS1 context, Λ has instead been called Λ_π , and is related to $\overline{M}_{Pl} = M_4/2$ of [16] by

$$\Lambda = \Lambda_\pi = e^{-\pi k R} \overline{M}_{Pl} . \quad (14)$$

III. THE SIGNAL

We now turn to a discussion of the intriguing possibility that a warped KK graviton G_1^* could be the source of the 750 GeV diphoton excess, and to other constraints on such a scenario. In this paper we focus on the simplest case where the SM is restricted to a brane at $y^m = 0$, as described above, although more general scenarios can be explored with Standard Model fields extending into the extra dimensions.

If a KK graviton is the source of the 750 GeV excess, this implies that the warping is significant, since in a pure large extra dimensions scenario[1, 14] there would be a near-continuum of KK excitations on these energy scales. As we have discussed, $m_1 = 750$ GeV is then related to a characteristic curvature scale of the extra dimensions; for the example of RS1 this would imply $k = 196$ GeV.

The remaining free parameter is Λ in (7), which can be fixed by matching to the signal cross section $\sigma(pp \rightarrow G_1^* \rightarrow \gamma\gamma)$. A 1.755 K -factor for 13 TeV, from the next-to-leading order (NLO) QCD corrections[17–20], is used in our work. We calculate the leading order (LO) graviton production cross section with MadGraph5 [21] with CT14llo parton distribution function (PDF) [22]. The renormalization scale (μ_R) and the factorization scale (μ_F) are fixed to be $\mu_R = \mu_F = 750$ GeV. Since we use the NLO QCD K -factor in calculating the inclusive cross section, the (renormalization and factorization) scale dependence uncertainty is estimated

to be suppressed to 9.3% [18]. The uncertainties from the choice of the PDFs are estimated by also performing calculations with CTEQ6L1[23] and MSTW2008LO PDFs[24]. We then find, including the combined uncertainties,

$$\sigma(pp \rightarrow G_1^*) = 7.74_{-1.10}^{+1.43} \text{pb} \times \left(\frac{10 \text{TeV}}{\Lambda} \right)^2 . \quad (15)$$

Here we estimate the central value by taking the algebraic average of the central values from the different PDFs, and the error region is the region covered by the scale uncertainties with different PDFs.

To fit the excess from the ATLAS collaboration, we generate parton level events using MadGraph5 [21] with CT14llo parton distribution function (PDF) [22]. $pp \rightarrow G_1^* + n j$ events are generated to $n=1$. The MLM matching scheme is used to avoid double counting in the parton showering [25]. All parton level events are showered using PYTHIA6.4 with Tune Z2 parameter assignment [26, 27]. We use DELPHES3 to mimic detector effects [28, 29]. More details of this fitting procedure can be found in [30, 31]. The best-fit result is shown in FIG. 1. The best-fit unfolded cross section from ATLAS is

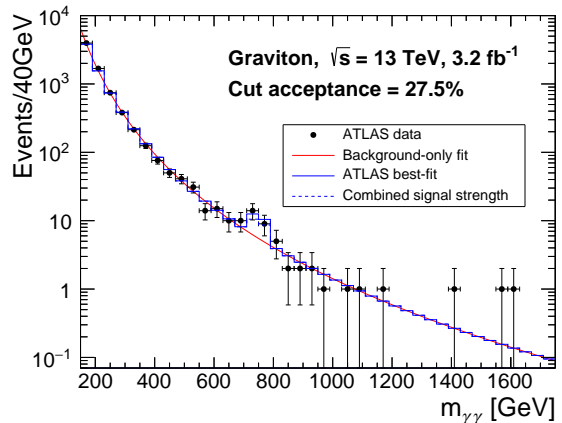


FIG. 1. The best-fit result to the 13 TeV LHC diphoton excess with a lightest KK graviton. The narrow width approximation is used in the fit. The solid blue line is our best-fit to the 13 TeV ATLAS data. The dashed blue line is the best-fit from a combination of the 13 TeV CMS results (from the CMS collaboration [3]) and our best-fit of the 13 TeV ATLAS data.

$\sigma(pp \rightarrow G_1^* \rightarrow \gamma\gamma) = 13.7_{-5.1}^{+5.9}$ fb. The cut acceptance from our simulation is 27.5% for a narrow width KK graviton.

A best-fit result to the 13 TeV CMS data ($\sigma = 6.6_{-3.3}^{+3.9}$ fb) was performed by the CMS collaboration. The best-fit result after combining the 13 TeV ATLAS and 13 TeV CMS results is $\sigma(pp \rightarrow G_1^* \rightarrow \gamma\gamma) = 9.3_{-2.9}^{+3.3}$ fb. The likelihood functions are shown in FIG. 2.

The partial decay widths of the KK graviton to SM particles via the Lagrangian (7) are given in [32]. The

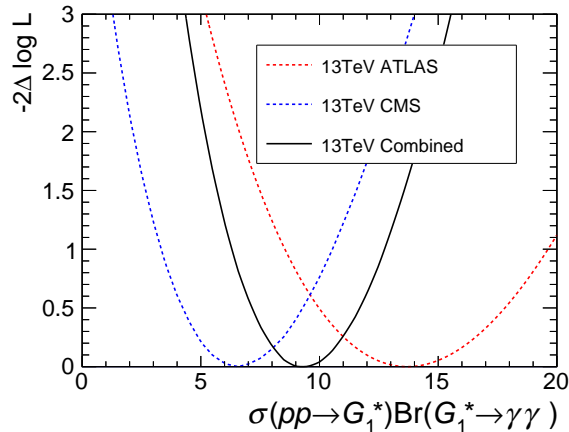


FIG. 2. The likelihood functions for the diphoton signal search. The likelihood function of the ATLAS excess is from our fit. The likelihood function of the CMS excess is extracted from the result presented in [3]. We combine these results to give the result with the black solid line. The best-fit cross section of the 13 TeV LHC is $\sigma(pp \rightarrow G_1^* \rightarrow \gamma\gamma) = 9.3_{-2.9}^{+3.3}$ fb.

partial decay width of the KK graviton to massless gauge bosons ($\Gamma_{V_0 V_0}$), massive gauge bosons (Γ_{VV}), fermions (Γ_{ff}) and the Higgs boson (Γ_{hh}) are

$$\Gamma_{V_0 V_0} = \frac{N_C m_1^3}{80\pi\Lambda^2} \quad (16)$$

$$\Gamma_{VV} = \delta \frac{m_1^3}{40\pi\Lambda^2} \left(1 - \frac{4m_V^2}{m_1^2}\right)^{1/2} \times \left(\frac{13}{12} + \frac{14m_V^2}{39m_1^2} + \frac{4m_V^4}{13m_1^4}\right), \quad (17)$$

$$\Gamma_{ff} = \delta \frac{N_C m_1^3}{160\pi\Lambda^2} \left(1 - \frac{4m_f^2}{m_1^2}\right)^{3/2} \left(1 + \frac{8m_f^2}{3m_1^2}\right), \quad (18)$$

$$\Gamma_{hh} = \frac{m_1^3}{480\pi\Lambda^2} \left(1 - \frac{4m_h^2}{m_1^2}\right)^{5/2}, \quad (19)$$

where N_C is a color factor which is 8 for gluons, 3 for quarks and 1 for colorless particles, and δ is 1/2 for self-conjugate particles and 1 for other particles. The total width of a 750 GeV KK graviton is then

$$\Gamma = 0.39\text{GeV} \times \left(\frac{10\text{TeV}}{\Lambda}\right)^2, \quad (20)$$

justifying the narrow-width approximation.

The decay branching ratio to the diphoton final state is (see FIG. 3)

$$\text{Br}(G_1^* \rightarrow \gamma\gamma) = 4.3\%, \quad (21)$$

As a result, the best-fit coupling scale from the ATLAS diphoton excess is

$$\Lambda_{\text{ATLAS}} \simeq 50_{-10}^{+12}\text{TeV} \quad (22)$$

and the CMS best-fit coupling scale is

$$\Lambda_{\text{CMS}} \simeq 71_{-18}^{+22}\text{TeV}. \quad (23)$$

If we consider the combined results, the best-fit coupling scale is

$$\Lambda_{\text{combined}} \simeq 60_{-10}^{+12}\text{TeV}. \quad (24)$$

The PDF uncertainties and statistical uncertainty are combined independently in these error estimates.

If a warped KK graviton couples with this strength, one also expects signals in other channels[5, 12]. Therefore, we next turn to an examination of constraints from other LHC data.

IV. CONSTRAINTS FROM LHC RUN-I

In this section, we examine constraints on a warped KK graviton from direct searches performed on LHC Run-I data. From the decay branching ratios of a 750 GeV KK graviton shown in FIG. 3, we find that the most important decay channel is the dijet channel where here the jets are associated with gluons and up, down, charm and strange quarks. The constraint from this channel is weak due to the huge SM background. The 8 TeV inclusive cross section of the 750 GeV KK graviton is calculated with MadGraph5 with the parameters and PDFs described in the last section. The result is (with the K -factor 1.922 [20], for 8 TeV)

$$\sigma(pp \rightarrow G_1^*) = 2.01_{-0.37}^{+0.47}\text{pb} \times \left(\frac{10\text{TeV}}{\Lambda}\right)^2. \quad (25)$$

In TABLE I, we list constraints from ATLAS and CMS at the 8 TeV LHC. The strongest constraint on Λ comes from the 8 TeV diphoton search by the CMS collaboration, which rule out the parameter range $\Lambda < 69$ TeV at 95% C.L. Thus the best-fit point to the 13 TeV ATLAS diphoton data is excluded by this result. However, the CMS best-fit result and the combined fit result is still allowed within 1σ .

We can also consider the signal and bounds from ATLAS and CMS collaborations separately. The 8 TeV bound from ATLAS collaboration is $\Lambda > 63$ TeV from the dilepton channel. So the ATLAS signal is excluded by its 8 TeV result. The 8 TeV bound from the CMS collaboration is $\Lambda > 69$ TeV from the diphoton channel, so the best-fit result of the CMS signal is just at the exclusion bound. Again, if we consider the uncertainties from the PDFs, as shown in TABLE II, it is seen that the CMS best-fit and the combined result are certainly allowed within 1σ when these uncertainties are included. The 1σ ATLAS best-fit region is at the edge of the exclusive bound from the ATLAS 8 TeV results when we considered these PDF uncertainties.

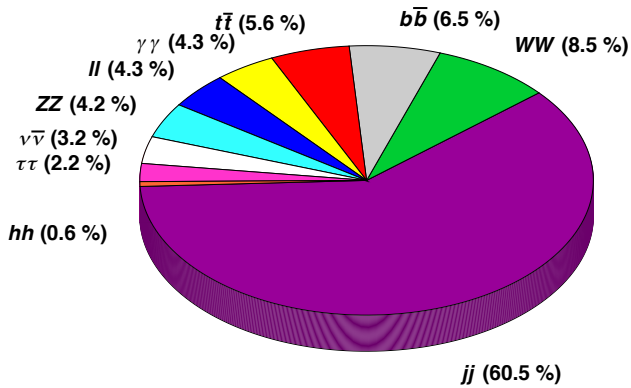


FIG. 3. The decay branching ratios of the 750 GeV KK graviton.

TABLE I. The constraints on $\sigma(pp \rightarrow G_1^*)$ at 8 TeV LHC (95% C.L. upper bound). The \mathcal{A} in the table is the cut acceptance of the process. The bounds for Λ shown in the last column are calculated using the central value of eq. (25).

	$\sigma(pp \rightarrow G_1^*)\text{Br}$ (pb)	$\sigma(pp \rightarrow G_1^*)$ (pb)	Λ (TeV)
jj	$1.25/\mathcal{A}$ [33]	$1.9/\mathcal{A}$	10.4
VV	0.065 [34] 0.055 [35]	1.2	13
$t\bar{t}$	0.52 [36], 0.4 [37]	7.8	5.1
$\gamma\gamma$	0.0024 [38], 0.0018 [39]	0.042	69
$\ell^+\ell^-$	0.0011 [40], 0.0014 [41]	0.051	63
$\tau^+\tau^-$	0.01 ^a [42]	0.47	21
hh	0.045 [43], 0.041 [44]	7.7	5.1

^a This is the constraint on a spin-1 particle. The spin-2 KK graviton will have a little larger cut acceptance and the exact constraint will be a little smaller but roughly the same.

TABLE II. The constraints on Λ at 8 TeV LHC (95% C.L. upper bound), with PDF uncertainties.

	jj	VV	$t\bar{t}$	$\gamma\gamma$	$\ell^+\ell^-$	$\tau^+\tau^-$	hh
Λ (TeV)	$10_{0.9}^{+1.2}\mathcal{A}$	$13_{-1.2}^{+1.5}$	$5.1_{-0.5}^{+0.6}$	69_{-6}^{+8}	63_{-6}^{+7}	21_{-2}^{+2}	$5.1_{-0.5}^{+0.6}$

V. CONSTRAINTS FROM LHC RUN-II

One should also examine the dilepton constraints from the 13 TeV LHC on a warped KK graviton. Both ATLAS and CMS collaborations search for an exotic spin-1 resonance in the dilepton final state [45, 46]. The upper bounds are summarized in TABLE III. To give a constraint for a graviton, we generate the signal events by the same method as in Sec. III but require the graviton to decay into dileptons. We also simulate a 750 GeV Z' for comparison, and infer the graviton bounds using the ratio between the cut acceptances, which should suppress uncertainties. The ratios between graviton and Z'

TABLE III. The upper bounds on $\sigma(pp \rightarrow Z')\text{Br}(Z' \rightarrow \ell\ell)$ from the 13 TeV LHC. The unit in this table is fb.

Channel	ee	$\mu\mu$	combined
13 TeV ATLAS [45]	6.2	13.8	5.6
13 TeV CMS [46]	3.5	8.5	2.9

cut acceptances ($\epsilon_X^{\ell\ell}$) from our simulations are

$$\text{ATLAS: } R_{\mu\mu} = \frac{\epsilon_{G_1^*}^{\mu\mu}}{\epsilon_{Z'}^{\mu\mu}} = 1.12, \quad R_{ee} = \frac{\epsilon_{G_1^*}^{ee}}{\epsilon_{Z'}^{ee}} = 1.35, \quad (26)$$

$$\text{CMS: } R_{\mu\mu} = \frac{\epsilon_{G_1^*}^{\mu\mu}}{\epsilon_{Z'}^{\mu\mu}} = 1.16, \quad R_{ee} = \frac{\epsilon_{G_1^*}^{ee}}{\epsilon_{Z'}^{ee}} = 1.23. \quad (27)$$

The cut acceptances for the graviton are larger than for the Z' due to the final state leptons being more central in the detector on average, which was also noted for the 8 TeV LHC (e.g., see Ref [41]). The strongest constraints are from the ee -channel. We show the constraints on a warped KK graviton from such 13 TeV dilepton searches in TABLE IV. We only show the result with CT14llo PDF since the constraints here are also from the 13 TeV LHC. We see from the result that the combined best-

TABLE IV. The bounds on $\sigma(pp \rightarrow G_1^*)\text{Br}(G_1^* \rightarrow \gamma\gamma)$ and Λ at 13 TeV LHC.

Channel	ATLAS (ee)	ATLAS ($\mu\mu$)	CMS (ee)	CMS ($\mu\mu$)
σ (fb)	9.2	24.6	5.7	14.7
Λ (TeV)	60	37	76	48

fit result from the 13 TeV ATLAS and 13 TeV CMS diphoton data is nearly excluded by the 13 TeV dilepton constraints (CMS ee channel), at 98% C.L. The best-fit result from the ATLAS signal is excluded by the 13 TeV CMS dielectron channel with 98.8% C.L., and excluded by the 13 TeV ATLAS dielectron channel with 96.8% C.L. The best-fit result from the 13 TeV CMS diphoton data is however (with less than 1σ uncertainty) still consistent with the 13 TeV dilepton constraints.

The CMS report[3] also combines the 8 TeV results with the 13 TeV results. The best-fit to the combined 8 TeV and 13 TeV CMS diphoton data is

$$\sigma(pp \rightarrow G_1^* \rightarrow \gamma\gamma) = 4.5_{-1.7}^{+1.9} \text{ fb}, \quad (28)$$

$$\Lambda = 86_{-17}^{+20} \text{ TeV}, \quad (29)$$

which is consistent with the constraint from the 13 TeV LHC dilepton data.

We also conclude from this discussion that if the 750 GeV excess is confirmed by the next round of data, and its source is a KK graviton in the simple type of warped compactification that we have considered, the resonance

should also be found very soon in the dilepton channel.⁴

VI. DISTINGUISHING THE GRAVITON FROM A SPIN-0 RESONANCE

It is well known that the final state diphoton angular distribution can be used to investigate the spin of a resonance. In this section, we estimate the luminos-

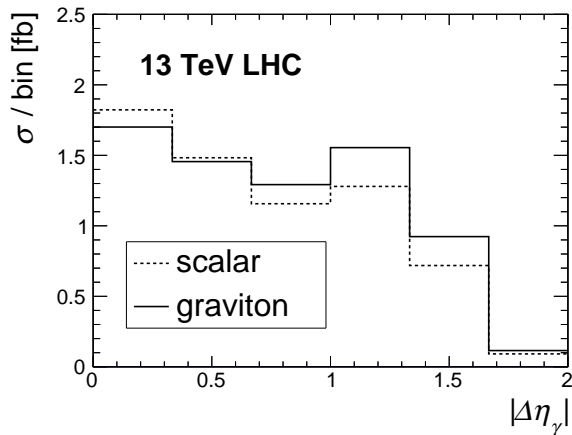


FIG. 4. The best-fit results for the LHC Run-II diphoton excess with the lightest KK graviton. We use the narrow width approximation.

ity which is needed to measure the spin of this diphoton resonance. For an (optimistic) example we assume the signal strength is the best-fit value to the ATLAS excess. In this preliminary estimate, we only generate the $pp \rightarrow \gamma\gamma$ SM background events with at most one additional jet with MadGraph5, PYTHIA6.4 and MLM matching scheme. The background strength is rescaled to the ATLAS background. In addition to the cuts used by the ATLAS collaboration [2], we require that the diphoton invariant mass satisfy

$$|m_{\gamma\gamma} - 750 \text{ GeV}| < 40 \text{ GeV}. \quad (30)$$

The distribution of the difference between the pseudorapidity of the leading and subleading photons in each event is shown in FIG. 4. To distinguish a spin-2 resonance from a spin-0 resonance with 99% C.L., roughly 50 fb^{-1} integrated luminosity is needed at 13 TeV. Of course, assuming the excess persists, more data will be needed to distinguish between spin 0 and spin 2 if the estimated signal cross section decreases. Note that the CMS collaboration separates their events into the “EBEE” (containing photon pairs where both candidates are reconstructed in the electromagnetic calorimeter (ECAL)

barrel) and “EBEE” (containing photon pairs where one of the candidates is reconstructed in the ECAL endcaps) categories. Their data shows that there is a significant (in fact, more) contribution to the signal from the EBEE category. This could hint that a spin-2 resonance is favored by the excess, but more data is needed to draw a conclusion.

VII. RELATING PHENOMENOLOGICAL TO FUNDAMENTAL PARAMETERS

As we have described, measurement of the mass of the lightest KK graviton can be thought of as determining a typical curvature radius scale of the extra-dimensional geometry. As a specific example, eq. (12) shows that a mass of 750 GeV fixes $k = 196 \text{ GeV}$ in RS1.

The strength of the signal, parameterized by Λ , is a combination of the higher-dimensional Planck mass, and the scale r_1 determining the density of the wavefunction in the extra dimensions, as in (8). If r_1 is the same scale as $1/m_1$, as might be typically expected, this then determines M_D . Specifically, in the example of RS1, this happens through (13), which with $\Lambda = 60 \text{ TeV}$, determines $M_5 = 33 \text{ TeV}$.

Finally, the warped volume is then determined by the ratio M_4/M_D , as in (2). In the RS1 example this becomes (11), which determines $kR \simeq 9.7$.

VIII. MODULI AND RADION

In general warped compactifications, there will also be light scalar fields arising from deformations of the compact metric g_{ab} which correspond to moduli. In general, the dynamics of the extra dimensions must provide a potential that gives mass to these deformations, for realistic phenomenology. We won’t consider the full story of such moduli, which can be complicated, here, but instead briefly illustrate such considerations in the toy model of RS1.

In RS1 there is a single light scalar radion arising from the yy component of the metric. A simple stabilization mechanism was introduced by Goldberger and Wise in [47]. This gave a radion mass which is determined in terms of k and R , as well as certain dimension 3/2 vacuum expectation value (vev) parameters v_h, v_v , as[48]

$$m_{rad} = \frac{v_v}{\sqrt{3}\pi M_5^{3/2}} \frac{1}{R} \log\left(\frac{v_h}{v_v}\right) \quad (31)$$

(here v_v, v_h are rescaled compared to [48]); corrections including back reaction are given in [49]. Since $kR \sim 10$ to generate the hierarchy, a subplanckian vev scale[47] $v_v/M_5^{3/2} < 1$ implies a radion mass in Goldberger/Wise-stabilized RS1 that is well below that of the KK graviton; with the parameters inferred above, we find $m_{rad} \lesssim 4 \text{ GeV}$. Searches for such a radion provide another test for

⁴ Alternately, non-trivial bulk structure of the SM fermions in a more complicated scenario could alter this result; see the discussion below.

such warped compactifications, though it is difficult to make precise and general statements for the general such compactification, where moduli phenomenology depends on the details of the stabilization mechanism.

To illustrate the phenomenology of the radion ϕ , consider the case where it couples to gravity only minimally. Its interaction with SM fields is given by[49]

$$\mathcal{L}_{\text{radion}} = \frac{\gamma\phi}{v} T_{\mu}^{\mu}, \quad (32)$$

where $v = 246$ GeV is the vev of the SM Higgs field, and $\gamma = v/(\sqrt{6}\Lambda) \simeq 1.6 \times 10^{-3}$. Thus, the coupling is quite weak. After electroweak symmetry breaking, one finds that[50]

$$\begin{aligned} T_{\mu}^{\mu} = & \sum_f m_f \bar{f} f - 2m_W^2 W_{\mu}^{+} W^{-\mu} - m_Z^2 Z_{\mu} Z^{\mu} \\ & + (2m_h^2 h^2 - \partial_{\mu} h \partial^{\mu} h) + \frac{\beta_{\text{QCD}}(g_s)}{2g_s} G_{\mu\nu}^a G^{a,\mu\nu} \\ & + \frac{\beta_{\text{QED}}(e)}{2e} F_{\mu\nu} F^{\mu\nu}, \end{aligned} \quad (33)$$

where β_{QCD} and β_{QED} are the QCD and QED beta functions, respectively.

The dominant production channel for the radion at a hadron collider is via gluon-gluon fusion. For such a light radion, the strongest constraints are from exotic scalar searches from heavy meson decay processes, $M \rightarrow \gamma\phi \rightarrow \gamma f \bar{f}$ where $M = \Upsilon(nS), J/\psi$. From the expressions in [51] we find

$$\frac{\Gamma(M \rightarrow \gamma\phi)}{\Gamma(M \rightarrow e^{+}e^{-})} \lesssim 10^{-8} \quad (34)$$

for $m_{\text{radion}} < 4$ GeV and $M = \Upsilon(nS), J/\psi$. Such a tiny branching ratio is beyond current experimental sensitivity[52–57].

IX. STANDARD MODEL MATTER IN THE BULK

The SM particles might also propagate, or have non-trivial distributions, in some of the extra dimensions. For example, in the bulk RS model, the coupling strengths between the KK graviton and the SM particles are corrected by an overlap between the wavefunctions of the SM particles and the KK graviton in the extra dimensions [58]. Such corrections can be different for SM fermions ($C_{f\bar{f}G_1^*}$) and SM gauge bosons ($C_{VVG_1^*}$). If the

correction increases $C_{VVG_1^*}/C_{f\bar{f}G_1^*}$, the gluon-gluon initial state contributes more to graviton production, and the production rate at 8 TeV LHC is decreased relative to the discussion above. Hence, constraints from 8 TeV LHC data are weakened. Also, the G_1^* decay branching ratio to the dilepton final state would decrease. Then, the dilepton signal might be much weaker than the diphoton signal, and might not be observed at 13 TeV LHC in the near future. There is a lot of model-dependency on the extra-dimensional geometry in such more-complicated models, which makes precise prediction here more difficult.

X. SUMMARY AND CONCLUSIONS

We have found that a warped KK graviton, with a coupling strength given by a scale $\Lambda \simeq 60_{-10}^{+12}$ TeV, is consistent with the 750 GeV excess observed at ATLAS and CMS. Constraints from other channels, particularly the 13 TeV dilepton data, put pressure on such a result in the simplest warped compactification scenarios, but are not strongly inconsistent with it. Thus, if the signal continues to be observed in future data, confirmation of such a scenario should also readily come from the dilepton channel. The constraints and this prediction are weakened for more complex warped scenarios. But in either case, confirmation would also ultimately come from angular distributions.

In the event the current excess does not persist, the preceding discussion gives a simple parameterization of KK graviton phenomenology, based on a simplified model that derives from a general warped compactification scenario. We have outlined how phenomenological parameters are related to the fundamental ones of such a warped compactification, and to aspects of the higher-dimensional geometry. This discussion could thus be pertinent to unraveling such a signal in the event one is discovered at higher mass.

XI. ACKNOWLEDGMENTS

This work was supported in part by the U.S. DOE under Contract No. DE-SC0011702, and by Foundational Questions Institute (fqxi.org) grant FQXi-RFP-1507. We thank N. Craig and L.-T. Wang for helpful discussions, and especially J. Incandela for a number of valuable suggestions and discussions, and for comments on a draft of this paper.

[1] N. Arkani-Hamed, S. Dimopoulos, and G. R. Dvali, Phys. Lett. **B429**, 263 (1998), hep-ph/9803315.
 [2] Tech. Rep. ATLAS-CONF-2015-081, CERN, Geneva (2015), URL <http://cds.cern.ch/record/2114853>.

[3] Tech. Rep. CMS-PAS-EXO-15-004, CERN, Geneva (2015), URL <http://cds.cern.ch/record/2114808>.
 [4] L. Aparicio, A. Azatov, E. Hardy, and A. Romanino (2016), arXiv:1602.00949.

- [5] R. Franceschini, G. F. Giudice, J. F. Kamenik, M. McCullough, A. Pomarol, R. Rattazzi, M. Redi, F. Riva, A. Strumia, and R. Torre (2015), arXiv:1512.04933.
- [6] M. Low, A. Tesi, and L.-T. Wang (2015), arXiv:1512.05328.
- [7] M. T. Arun and P. Saha (2015), arXiv:1512.06335.
- [8] C. Han, H. M. Lee, M. Park, and V. Sanz (2015), arXiv:1512.06376.
- [9] J. S. Kim, K. Rolbiecki, and R. R. de Austri (2015), arXiv:1512.06797.
- [10] A. Martini, K. Mawatari, and D. Sengupta (2016), arXiv:1601.05729.
- [11] C.-Q. Geng and D. Huang (2016), arXiv:1601.07385.
- [12] K. A. Olive et al. (Particle Data Group), *Chin. Phys.* **C38**, 090001 (2014).
- [13] L. Randall and R. Sundrum, *Phys. Rev. Lett.* **83**, 3370 (1999), hep-ph/9905221.
- [14] I. Antoniadis, N. Arkani-Hamed, S. Dimopoulos, and G. R. Dvali, *Phys. Lett.* **B436**, 257 (1998), hep-ph/9804398.
- [15] S. B. Giddings and M. L. Mangano, *Phys. Rev.* **D78**, 035009 (2008), arXiv:0806.3381.
- [16] H. Davoudiasl, J. L. Hewett, and T. G. Rizzo, *Phys. Rev. Lett.* **84**, 2080 (2000), hep-ph/9909255.
- [17] P. Mathews, V. Ravindran, and K. Sridhar, *JHEP* **10**, 031 (2005), hep-ph/0506158.
- [18] Q. Li, C. S. Li, and L. L. Yang, *Phys. Rev.* **D74**, 056002 (2006), hep-ph/0606045.
- [19] M. C. Kumar, P. Mathews, V. Ravindran, and A. Tripathi, *Nucl. Phys.* **B818**, 28 (2009), arXiv:0902.4894.
- [20] J. Gao, C. S. Li, B. H. Li, C. P. Yuan, and H. X. Zhu, *Phys. Rev.* **D82**, 014020 (2010), arXiv:1004.0876.
- [21] J. Alwall, R. Frederix, S. Frixione, V. Hirschi, F. Maltoni, et al., *JHEP* **1407**, 079 (2014), arXiv:1405.0301.
- [22] S. Dulat, T. J. Hou, J. Gao, M. Guzzi, J. Huston, P. Nadolsky, J. Pumplin, C. Schmidt, D. Stump, and C. P. Yuan (2015), arXiv:1506.07443.
- [23] J. Pumplin, D. R. Stump, J. Huston, H. L. Lai, P. M. Nadolsky, and W. K. Tung, *JHEP* **07**, 012 (2002), hep-ph/0201195.
- [24] A. D. Martin, W. J. Stirling, R. S. Thorne, and G. Watt, *Eur. Phys. J.* **C63**, 189 (2009), arXiv:0901.0002.
- [25] M. L. Mangano, M. Moretti, F. Piccinini, and M. Trecani, *JHEP* **01**, 013 (2007), hep-ph/0611129.
- [26] T. Sjostrand, S. Mrenna, and P. Z. Skands, *JHEP* **0605**, 026 (2006), hep-ph/0603175.
- [27] R. Field, *Acta Phys. Polon.* **B42**, 2631 (2011), arXiv:1110.5530.
- [28] J. de Favereau et al. (DELPHES 3), *JHEP* **1402**, 057 (2014), arXiv:1307.6346.
- [29] M. Cacciari, G. P. Salam, and G. Soyez, *Eur. Phys. J.* **C72**, 1896 (2012), arXiv:1111.6097.
- [30] J. Gao, H. Zhang, and H. X. Zhu (2015), arXiv:1512.08478.
- [31] H. Zhang (2016), arXiv:1601.01355.
- [32] T. Han, J. D. Lykken, and R.-J. Zhang, *Phys. Rev.* **D59**, 105006 (1999), hep-ph/9811350.
- [33] G. Aad et al. (ATLAS), *Phys. Rev.* **D91**, 052007 (2015), arXiv:1407.1376.
- [34] G. Aad et al. (ATLAS) (2015), arXiv:1512.05099.
- [35] Tech. Rep. CMS-PAS-EXO-12-022, CERN, Geneva (2013), URL <https://cds.cern.ch/record/1596494>.
- [36] G. Aad et al. (ATLAS), *JHEP* **08**, 148 (2015), arXiv:1505.07018.
- [37] V. Khachatryan et al. (CMS), *Phys. Rev.* **D93**, 012001 (2016), arXiv:1506.03062.
- [38] G. Aad et al. (ATLAS), *Phys. Rev.* **D92**, 032004 (2015), arXiv:1504.05511.
- [39] Tech. Rep. CMS-PAS-EXO-12-045, CERN, Geneva (2015), URL <http://cds.cern.ch/record/2017806>.
- [40] G. Aad et al. (ATLAS), *Phys. Rev.* **D90**, 052005 (2014), arXiv:1405.4123.
- [41] V. Khachatryan et al. (CMS), *JHEP* **04**, 025 (2015), arXiv:1412.6302.
- [42] G. Aad et al. (ATLAS), *JHEP* **07**, 157 (2015), arXiv:1502.07177.
- [43] G. Aad et al. (ATLAS), *Phys. Rev.* **D92**, 092004 (2015), arXiv:1509.04670.
- [44] V. Khachatryan et al. (CMS), *Phys. Lett.* **B749**, 560 (2015), arXiv:1503.04114.
- [45] Tech. Rep. ATLAS-CONF-2015-070, CERN, Geneva (2015), URL <http://cds.cern.ch/record/2114842>.
- [46] Tech. Rep. CMS-PAS-EXO-15-005, CERN, Geneva (2015), URL <http://cds.cern.ch/record/2114855>.
- [47] W. D. Goldberger and M. B. Wise, *Phys. Rev. Lett.* **83**, 4922 (1999), hep-ph/9907447.
- [48] W. D. Goldberger and M. B. Wise, *Phys. Lett.* **B475**, 275 (2000), hep-ph/9911457.
- [49] C. Csaki, M. L. Graesser, and G. D. Kribs, *Phys. Rev.* **D63**, 065002 (2001), hep-th/0008151.
- [50] S. Bae, P. Ko, H. S. Lee, and J. Lee, *Phys. Lett.* **B487**, 299 (2000), [C21(2000)], hep-ph/0002224.
- [51] P. Nason, *Phys. Lett.* **B175**, 223 (1986).
- [52] W. Love et al. (CLEO), *Phys. Rev. Lett.* **101**, 151802 (2008), arXiv:0807.1427.
- [53] J. P. Lees et al. (BaBar), *Phys. Rev. Lett.* **107**, 221803 (2011), arXiv:1108.3549.
- [54] J. P. Lees et al. (BaBar), *Phys. Rev.* **D87**, 031102 (2013), [Erratum: *Phys. Rev.* **D87**, no.5, 059903 (2013)], arXiv:1210.0287.
- [55] J. P. Lees et al. (BaBar), *Phys. Rev.* **D88**, 031701 (2013), arXiv:1307.5306.
- [56] J. Lees et al. (BaBar), *Phys. Rev.* **D91**, 071102 (2015), arXiv:1502.06019.
- [57] M. Ablikim (BESIII) (2015), arXiv:1510.01641.
- [58] H. Davoudiasl, J. L. Hewett, and T. G. Rizzo, *Phys. Rev.* **D63**, 075004 (2001), hep-ph/0006041.